Shear and compression characteristics of peanut vines based on response surface methodology

Yong Chen[1], Ruonan Mao[1], Xiuli Zhang[1*], Hao Ma[2], Bingjun Li[1], Bin Hu[3], Xin Luo[3], Jiahui Zhao[1], Xiaochan Liu[1]

(1. *College of Mechanical and Electrical Engineering, Henan Agricultural University, Zhengzhou 450002, China*; 2. *College of Agricultural Equipment Engineering, Henan University of Science and Technology, Luoyang 471003, Henan, China*; 3. *College of Mechanical and Electrical Engineering, Shihezi University, Shihezi 832000, Xinjiang, China*)

Abstract: To address issues such as incomplete shredding and high energy consumption during peanut vine processing, this study investigated the mechanical properties of peanut vines. This study employed the response surface methodology to systematically investigate the shear and compressive mechanical properties of peanut vines under varying sampling locations, loading rates, and moisture contents. The results indicated that the root base of peanut vines exhibited the strongest shear and compressive resistance, with an average maximum shear force of 46.44±1.70 N, ultimate load of 26.90 N, fracture strength of 0.39 MPa, and elastic modulus of 3.52 MPa. A novel finding is the bimodal characteristic of the shear force-displacement curve, indicating two distinct failure stages involving both the rind and the pith cavity. Furthermore, moisture content negatively correlates with shear strength. Response surface analysis revealed that both shear location and moisture content significantly affected the shear force of peanut vines, with shear location having the most pronounced influence. Within the quasi-static loading range examined, the shear force reached its maximum when the cutting point was at the root, the loading speed was 40 mm/min, and the moisture content was 30% for peanut vines. This study provides a theoretical basis and benchmark data support for the development of efficient peanut vine shredding technology.

Keywords: peanut vines, shear force, compression characteristics, mechanical properties, Box-Behnken response surface analysis

DOI: 10.25165/j.ijabe.20261904.10439

Citation: Chen Y, Mao R N, Zhang X L, Ma H, Li B J, Hu B, et al. Shear and compression characteristics of peanut vines based on response surface methodology. Int J Agric & Biol Eng, 2026; 19(4): 328–337.

1 Introduction

According to national statistics, Henan Province's total peanut production reached 638.22×10³ t in 2024 and 647.58×10³ t in 2025, representing a year-over-year increase of 1.47%[1]. Peanut vines are rich in nutrients and inexpensive[2]. Crawling peanut vines contain 15.5% crude protein, 2.7% crude fat, and 45.8% carbohydrates. In animal husbandry, they can partially replace high-quality protein feed and coarse feed resources[3-5]. Their efficient utilization significantly reduces farming costs. The key to achieving feed utilization lies in effective grinding operations[6,7]. Superior grinding results markedly enhance feed palatability, digestibility, and subsequent deep processing efficiency[8]. However, in the current mechanized harvesting of peanuts, there are widespread issues such as incomplete shredding of excessively long and thick peanut stalks, as well as high energy consumption[9,10]. Therefore, to enhance the crushing efficiency and quality of peanut vines during the crushing process, this study investigated the shear and compression mechanical properties of peanut vines[11].

Currently, scholars both domestically and internationally have conducted extensive research on the shear and compression physical and mechanical properties of agricultural materials. Chahal et al.[12] conducted mechanical property tests on the wood-bark interface of shrub willow. Shear tests under quasi-static conditions revealed their stress-strain behavior, aiding in the design and optimization of debarking equipment for short rotation woody crops. Shi et al.[13] investigated the mechanical properties of Artemisia annua stems, conducting compression, shear, and bending tests on samples of two different diameters and stem sections. The tests revealed that the radial shear force of the stems was significantly greater than the axial shear force. Furthermore, the peak shear force and shear work exhibited linear positive correlations with the cross-sectional area of the samples, while shear work showed an exponential positive correlation. These findings enabled more efficient harvesting methods. Ye et al.[14] conducted physical shear and compression tests on reed-like stems, obtaining a maximum stem shear force of 155.18 N. They established a flexible reed-like stem model and performed simulated shear and compression tests on this model. He et al.[15] conducted shear tests on peanut vine roots and stems based

Received date: 2026-01-09 **Accepted date:** 2026-07-28

Biographies: Yong Chen, PhD, Associate Professor, research interest: design and performance test of agricultural machinery, Email: chenyong@henau.edu.cn; **Ruonan Mao**, Master candidate, research interest: mechanization design, Email: 15713911335@163.com; **Hao Ma**, PhD, Associate Professor, research interest: non-destructive testing technology for agricultural crops, Email: mahao@haust.edu.cn; **Bingjun Li**, PhD, Professor, research interest: agricultural systems engineering, Email: zzlbjun@163.com; **Bin Hu**, PhD, Professor, research interest: agricultural machinery design and performance testing, Email: hb_mac@shzu.edu.cn; **Xin Luo**, PhD, Professor, research interest: computer-aided virtual simulation design, Email: lx_mac@shzu.edu.cn; **Jiahui Zhao**, Master candidate, research interest: mechanical principles, Email: 2771956451@qq.com; **Xiaochan Liu**, PhD, Lecturer, research interest: research and development of modern agricultural equipment and agricultural machinery dynamics, Email: liuxiaochan@henau.edu.cn.

***Corresponding author: Xiuli Zhang**, PhD, Professor, research interest: theory and method of agricultural equipment design. College of Mechanical and Electrical Engineering, Henan Agricultural University, Zhengzhou 450002, China. Tel: +86- 13938553090, Email: zhangxiuli619@126.com.

on their differing mechanical properties, and measured the recovery coefficients of peanut vine roots and stems. Liu et al.[16] investigated the shear and compressive mechanical properties of the yam root-soil composite. The shear process was divided into three stages: elastic deformation, plastic deformation, and complete failure. Axial compression and radial compression tests were conducted, and corresponding discrete element models were established. Coetzee et al.[17] studied maize kernels as materials, determining their internal friction angle and stiffness properties through shear tests and compression tests, respectively. They investigated the mechanical properties and critical state characteristics of maize root-soil composites at different soil depths. Ma et al.[18] concluded that the middle root-rich zone, where roots were most densely distributed, exhibited the highest shear strength and initial deformation modulus. Schramm et al.[19] calibrated model parameters using three-point bending tests, cantilever beam tests, and uniaxial compression tests on mature winter wheat straw. They validated the model's effectiveness in simulating wheat straw shear behavior through ASTM straight shear tests. Chen et al.[20] conducted shear and quasi-static compression tests on rice grains to elucidate the key mechanism of grain breakage during husking. Their research revealed that breakage during husking results from the combined effects of flexible compression and shear loading. Liang et al.[21] conducted research on Xinjiang cotton, measuring the angle of repose of chopped cotton stalks at different moisture contents through physical experiments. The aforementioned scholars have conducted extensive research on numerous agricultural materials, but there are currently few reports on the mechanical properties of peanut vines.

This study conducted shear tests on peanut vine samples, varying the sampling location, shear rate, and moisture content. Compression tests were also performed on peanut vine samples from different locations. The research investigated the influence patterns of these factors on the shear strength and compressive mechanical properties of peanut vines. Subsequently, a second-order response model was established using response surface methodology to clarify the interaction effects among these factors. This study aims to systematically investigate the quasi-static shear and compressive mechanical properties of peanut vines and reveal their relationships with factors such as sampling locations and moisture contents, thereby providing baseline data for the subsequent establishment of more realistic dynamic models and the optimization of shredding equipment.

2 Materials and methods

2.1 Test site, equipment, and materials

The experimental site was located at the College of Mechanical and Electrical Engineering, Henan Agricultural University. Field-grown peanut vines from Xinxiang City, Henan Province, were selected as experimental samples. The variety type was Huayu 28, and the sampling period was from September 30, 2025, to October 6, 2025. During sample collection, the cut ends of the peanut vines were wrapped with plastic film, and the samples were immediately transported to the laboratory for testing.

Fifty test specimens from the harvested peanut vines were prepared. The main stems selected were upright and non-lodging, free from pests and diseases, and exhibited minimal variation in diameter. Using pruning shears, the stems were cut close to the base and all branches and leaves were removed from the main stem[22]. The total length of peanut vine samples ranged from 30 cm to 40 cm. The following image shows a cross-section of peanut vines. As shown in Figure 1, peanut vines possessed dense cortex tissue and well-developed vascular bundles. As the sampling location moves toward the stem of the peanut vine, the pith cavity gradually enlarges, revealing a distinct hollow structure. The main stem of peanut vines exhibited angular ridges in its middle and upper sections, with an overall irregular circular outline. L_1 was selected as its maximum diameter, measured using a vernier caliper, yielding a length of 6.40±0.02 mm.

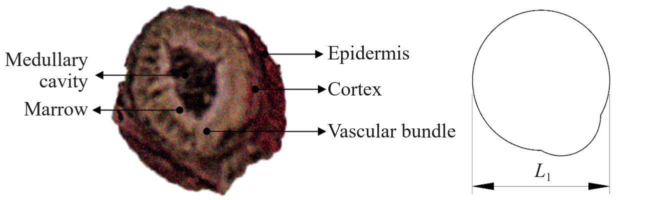

a. Cross-section of peanut vines b. Simplified diagram of peanut vines

Figure 1 Schematic diagram of peanut vine cutting cross-section

Instruments and equipment used during the test: WDW-1E electronic universal testing machine (Jinan Nair Testing Machine Co., Ltd.), AR224CN electronic balance (measurement accuracy 0.001 g), Model 101-1AB electric hot air circulating drying oven (Beijing Zhongxing Weiye Century Instrument Co., Ltd.), vernier caliper (measuring accuracy 0.02 mm), pruning shears, shear test tools, etc.

2.2 Test method

2.2.1 Moisture content determination

Peanut vines with robust main stems and free of diseases and pests were selected. The moisture content of the plants was measured by dividing them into three sections: top, middle, and root. When peanut vines reached 30-40 cm in length, as shown in Figure 2, they were cut at the base using pruning shears. For moisture content determination, samples were taken extending 20.0±0.5 mm outward from the center of each section[23]. According to national standard GB/T 1931-2009, five samples were grouped together for testing (groups A, B, and C, where group A consisted of top samples, group B of middle samples, and group C of root samples). The average masses of samples in groups A, B, and C were approximately 2.67 g, 3.16 g, and 3.13 g, respectively. Samples from the same batch were placed in an electric hot-air drying oven and dried at 105°C for 8 h. Subsequently, two to three samples were selected for weighing. Thereafter, the selected samples were weighed every 2 h until no further change in mass occurred, indicating the completion of drying[24]. The experiment was repeated five times, and the average value was taken.

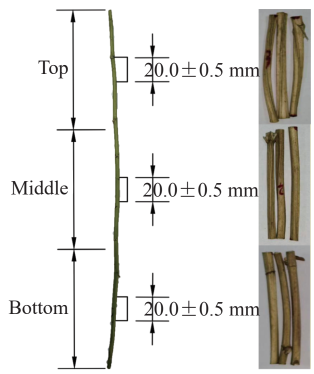

Figure 2 Schematic diagram of sampling zones for determining moisture content in the main stems of peanut vines

The moisture content of groups A, B, and C is calculated according to Equation (1), accurate to 0.1%.

$$W = \frac{m_1 - m_0}{m_0} \times 100\% \tag{1}$$

In the formula, W is the moisture content of the sample, %; m_1 is the mass of the wet sample, g; m_0 is the mass of the dry sample, g.

Calculations indicated that the average moisture content of peanut vines at the top (group A) was 82.3%, the middle section (group B) was 79.9%, and the root section (group C) was 76.1%. The moisture content of different parts of peanut vines ranged between 70% and 85%, indicating that peanut vines had relatively high moisture content.

2.2.2 Peanut vines shear test

Firstly, pruning shears were used to remove lateral branches and leaf buds from the collected peanut vines. Each vine was divided into three equal sections based on height: top, middle, and root. From the center of each section, a sample was cut extending outward on both sides, with a total length of 20.0±0.5 mm. The moisture content of peanut vines ranged between 75% and 85%, as shown in Figure 3. The specimens were then subjected to shear testing.

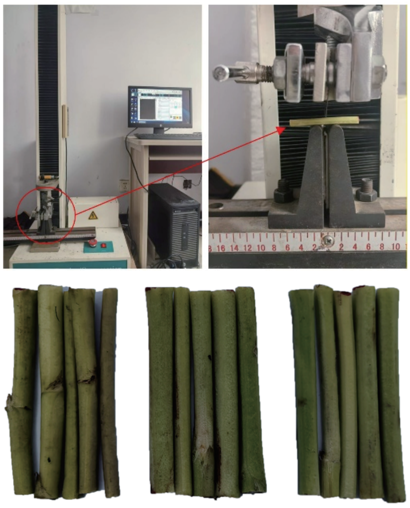

Figure 3 Shear test bench and shear specimens

Before testing, the shear tool was clamped onto the universal testing machine. A peanut vine specimen was secured on the shear platform and the machine was started to adjust the tool height. Loading was paused when the descending tool just contacted the peanut vine. The fixture and specimen position were adjusted to align the peanut vine vertically with the tool head[25]. During testing, the blade was driven at the preset loading speed to shear the peanut vine. The monitored parameters were displayed on the control console. When the shear curve displayed a distinct inflection point and shear force decreased, indicating shear failure of the peanut vine, the current shear test was immediately stopped[26].

During peanut vine shear testing, to maintain the shear test within a quasi-static range, three loading speeds were set at 30 mm/min, 40 mm/min, and 50 mm/min. Each group comprised five samples to investigate the variation patterns of peanut vine shear force at different speeds. Subsequently, peanut vines were divided into distinct sections based on their top, middle, and root portions (groups A_1, groups B_1, and groups C_1). Samples from each section were trimmed to a length of 50.0±0.5 mm and subjected to shear testing at a rate of 30 mm/min using a universal testing machine to further investigate the influence of different sections on the shear force of peanut vines. Figure 4 below shows cross-sectional views of the root, middle section, and top of peanut vines. Finally, peanut vine samples were soaked in clean water for 24 h. After soaking, they were placed in an electric hot-air drying oven for drying at a temperature of 45°C. This controlled the moisture content of different parts of the peanut vine samples to 30%, 40%, and 50%, respectively, to investigate the effect of moisture content on the shear force of peanut vines[27,28].

a. Root cross-section b. Central cross-section c. Top cross-section

Figure 4 Cross-section of peanut vines

2.2.3 Peanut vines compression test

Compressed peanut vine specimens were prepared to a length of 15.0±0.5 mm. Based on the average diameters of the top, middle, and root sections (0.384 cm, 0.492 cm, and 0.465 cm respectively), the specimens were categorized into groups A_2, groups B_2, and groups C_2. The moisture content of all three groups of peanut vine specimens ranged between 75% and 85%. The peanut vine specimens were placed on the test platform. A 30 mm diameter indenter was positioned at a distance of 1 mm to 2 mm from the specimen. The universal testing machine performed the compression test at a downward speed of 30 mm/min[29]. During compression, loading was stopped when the compressive force exhibited a gradual decrease and the specimen showed deformation under pressure. The compression test platform and specimen setup are illustrated in Figure 5.

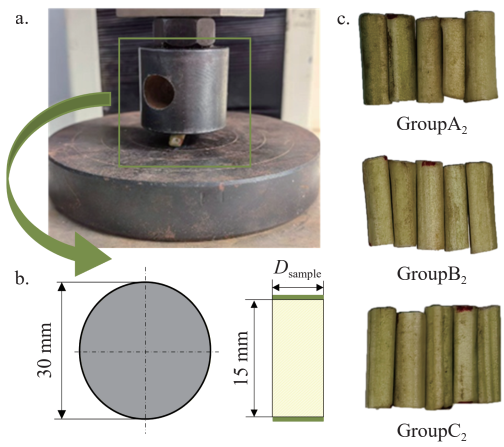

Note: a. Compression testing platform b. Schematic diagram of contact area and sample dimensions c. Peanut vine compression test samples

Figure 5 Compression test bench and compression specimen

During compression testing, the curve and ultimate load were recorded for each specimen. The diameter of each specimen group was measured and their breaking strength and elastic modulus were calculated. The mechanical response and deformation characteristics of peanut vines under axial pressure were systematically evaluated[30].

Compressive strength refers to the maximum yield strength achieved by peanut vines under compression, representing their resistance to crushing during compression testing. This is calculated using Equation (2), while Equation (3) is used to determine the elastic modulus of peanut vines[31].

$$\sigma = \frac{F_N}{A_1} \tag{2}$$

$$E = \frac{F_N \times L}{A_1 \times \Delta L} \tag{3}$$

In the formula, σ is the compressive strength of peanut vines, MPa; F_N is the maximum compressive force, N; A_1 is projected contact area, mm^2; E is the elastic modulus of peanut vines, MPa; L is the effective length of the specimen, mm; ΔL is the maximum compression displacement, mm.

In this experiment, the indenter diameter was 30 mm, and the length of the peanut vine specimen was 15 mm. Since the indenter width was greater than the specimen length and the load direction was perpendicular to the specimen axis, the contact area between the peanut vine and the indenter was approximately rectangular. The length of the specimen (D_{sample}) was taken as 15 mm, and the width was taken as the outer diameter of the specimen. Therefore, the compression area A_1 was calculated using Equation (4):

$$A_1 = L_{sample} \times D_{sample} \tag{4}$$

In the formula, L_{sample} is the length of the peanut vine sample, and D_{sample} is the outer diameter of the peanut vine sample.

3 Results and analysis

3.1 Effect of different shear rates on the shear force of peanut vines

Within the quasi-static loading range, the universal testing machine was set to three speed levels: 30 mm/min, 40 mm/min, and 50 mm/min. Shear force was applied to the peanut vine until the cut surface fractured and the test stopped. Table 1 lists the maximum shear force exerted on peanut vines at three different speeds and the corresponding displacement values. Each group underwent five trials, and the average values were recorded. As shown in the table data, the maximum shear force of peanut vines exhibited a clear increasing trend with increasing shear rate.

At a speed of 30 mm/min, the maximum shear force on peanut vines ranges between 18.614 N and 35.478 N, with an average maximum shear force of 28.240 N. When the speed increases to 40 mm/min, the average maximum shear force rises slightly to 30.138 N. At the higher speed of 50 mm/min, the average maximum shear force significantly increases to approximately 46.614 N. Meanwhile, the displacement values at shear failure remain relatively stable across different speeds, averaging 3.86 mm, 3.18 mm, and 4.46 mm, respectively. The data indicate that shear speed is a key factor influencing the shear force of peanut vines.

It should be noted that the loading rates used in this study fall entirely within the quasi-static regime. Therefore, the results in this section serve only as low-speed baseline data, and future dynamic impact tests are required to fully characterize the real-world shredding process.

3.2 Effect of different shear locations on the shearing force of peanut vines

Subsequently, specimens measuring 15.0±0.5 mm were taken from the root, middle, and top sections of peanut vines as shear test specimens. After shearing begins, the initial stage is elastic deformation, where the shear force-displacement curve rises nearly linearly from the origin. At this point, the tool has just contacted the peanut vine, and the applied pressure causes elastic compression of the vine. This is followed by the yield stage. When the accumulated shear force exceeds the strength limit of the peanut vine’s outer skin, the vine yields. This marks the attainment of the peak shear force.

After severing the main body, the tool interacts with the softer spongy pith inside the peanut vine and the opposite side wall, causing the shear force to continue increasing until the peanut vine breaks. As a result, the shear force-displacement curve exhibits two peaks during shear testing of peanut vines. To better analyze the influence of different shear locations on the shear force of peanut vines, this study employs a Gaussian model to fit the shear force-displacement curves for the root, middle section, and top of the vines. The fitting results are shown in Figure 6.

Table 1 Maximum shear force versus displacement at different speeds

Sample	30 mm/min		40 mm/min		50 mm/min	
Sample type	Maximum/N	Displacement/mm	Maximum/N	Displacement/mm	Maximum/N	Displacement/mm
1	25.591	4.20	35.611	3.30	42.363	4.22
2	32.794	4.60	25.683	2.70	47.071	4.32
3	18.614	2.70	29.589	3.40	50.099	4.71
4	28.723	4.00	28.041	3.40	47.739	4.68
5	35.478	3.80	31.766	3.10	45.799	4.36
Mean	28.240	3.86	30.138	3.18	46.614	4.46

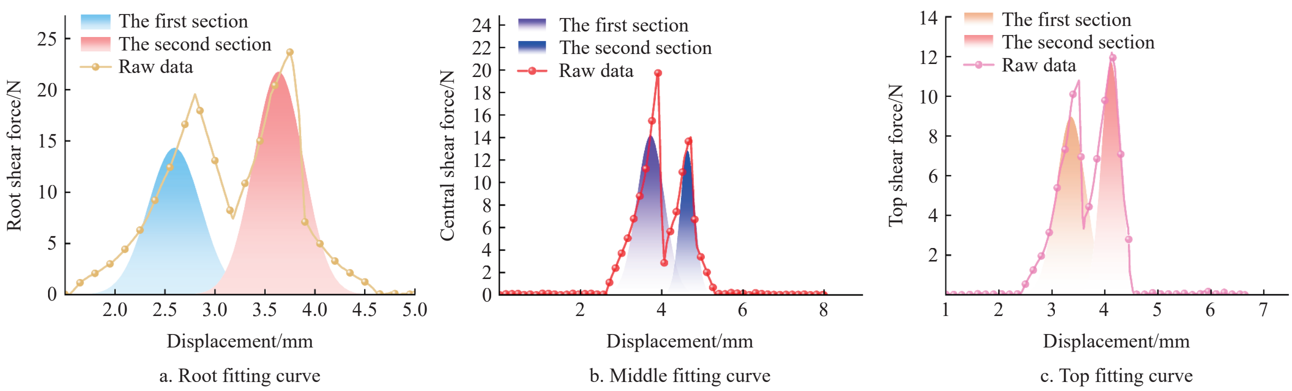

Figure 6 Fitting diagram of shear force-displacement curves for peanut vine roots at the base, middle, and top sections

The Gaussian distribution, also known as the normal distribution, is a common probability distribution[32]. To accurately describe the bimodal characteristics observed in the shear stress-displacement curves for different regions, this study fits the experimental data using a model consisting of two superimposed Gaussian functions, as shown in Equation (5):

$$p(x)=\frac{1}{\sqrt{2\pi\sigma^2}}e^{-\frac{(x-\mu)^2}{2\sigma^2}} \quad (5)$$

where, σ^2 denotes the variance, and μ represents the mean.

$$F(x)=A_1\exp\left(-\frac{(x-\mu_1)^2}{w_1}\right)+A_2\exp\left(-\frac{(x-\mu_2)^2}{w_2}\right)+y_0 \quad (6)$$

where, A_1 and A_2 represent the amplitudes of the two peaks, μ_1 and μ_2 represent the peak positions, w_1 and w_2 represent the peak width parameters, and y_0 represents the baseline offset.

The model can describe the mechanical processes of two mechanical stages—i.e., the rupture of the outer layer and the involvement of medullary cavity in shearing—corresponding to the first and second peaks, respectively. Using nonlinear fitting algorithm in Origin software, a double-Gaussian superposition fit was performed on the experimental data based on the least squares method, yielding the fitting parameters for each region (Table 2).

Table 2 Gaussian fitting model parameters

Sample type	Gaussian fitting parameters							
Shear location	Peak 1				Peak 2			
	y_0	x_c	A_1	w_1	y_0	x_c	A_2	w_2
Root	0	2.5938	9.5043	0.6228	0	3.6349	13.6297	0.5884
Middle	0	3.7241	12.2128	0.8076	0	4.6325	5.9309	0.4332
Top	0	3.3596	6.2649	0.6555	0	4.1139	5.3690	0.4299

Note: The parameters to be evaluated, A, x_c, and w, represent the peak amplitude, peak position, and half-width information of the Gaussian curve, respectively. In this study, since the shear force is 0 when there is no shear, it is set to 0 here.

The coefficient of determination R^2 is a statistical measure used to assess the goodness of fit of a regression model. The closer R^2 is to 1, the better the fit. The R^2 values for the three fitted models are 0.906, 0.924, and 0.971, respectively. The fitting results indicate that the Gaussian model exhibits superior fitting accuracy. Analysis of the fitted curves reveals that the shear force-displacement curves for the root, middle, and top sections all exhibit a bimodal characteristic. This indicates that each section undergoes two distinct stages of mechanical response during the shearing process, suggesting that the pith cavity within the central column of peanut vines also participates in the shearing action.

Figure 6 illustrates the dynamic response characteristics of shear force versus displacement for the root, middle, and top sections of peanut vines during shear testing, and characterizes the bimodal behavior using a superimposed double-Gaussian model. From the overall trend, all three subplots exhibit distinct bimodal shear characteristics, which are closely related to the non-uniform anatomical structure of the peanut vine and the sequential failure of different fiber layers. During the initial stage of the test—the first segment of the curve—the shear force for all three sample groups remains stable and approaches zero over a displacement range that closely follows the horizontal axis. This phenomenon has clear physical significance, corresponding to the idle travel phase where the shear tool contacts the reference surface and moves toward the sample. The steady zero-force output during this phase strongly validates the initial calibration and stability of the testing system. Subsequently, as the shear tool penetrates the vine, the shear force begins to rise sharply. The raw data points in Figures 6a-6c fully record the complete fluctuation of the force as a function of displacement.

Comparing the three areas, in the shear force-displacement curve of peanut root systems, two peaks are observed near displacements of 2.593 mm and 3.634 mm, respectively. The amplitude of the second peak is significantly higher than that of the first, indicating enhanced secondary structural load-bearing capacity in the root system. The peak positions of the mid-section curve in peanut vines occur at 3.724 mm and 4.632 mm, with the overall response shifting to the right compared to the root section and exhibiting significantly increased shear force. The two peaks of the top curve are located at 3.369 mm and 4.113 mm, with their positions and amplitudes falling between those of the root and mid-sections.

Following bimodal shear failure, the curve drops rapidly at the end and returns to a stable baseline phase approaching zero. This indicates that the fiber structure of the peanut vine has been completely sheared and separated; once the blade penetrates the sample, it encounters no further mechanical resistance. Furthermore, the sharp drop to zero at the end of the data confirms that the shear failure is complete, with no fiber entanglement. At the same time, the shaded regions of the Gaussian segmented fitting curves for the first and second stages in the figure exhibit an extremely high degree of overlap with the original experimental data points. This not only accurately captures the evolution of the bimodal pattern but also provides robust data support for quantitatively evaluating the goodness of fit during the shearing process.

Table 3 presents the overall mean maximum shear force and standard deviation for peanut vine samples across three distinct shear locations, derived from five replicate groups (n=5 per group, totaling n=25 per location). Among these locations, the root section exhibited the highest mechanical resistance, with a mean maximum shear force of 46.44±1.70 N. This indicates a stronger load-bearing capacity and greater structural stiffness in the basal region. In contrast, the middle section showed intermediate values 35.53±1.41 N, while the top section recorded the lowest shear force 25.29±0.51 N, reflecting its relatively compliant mechanical properties. Overall, the mean maximum shear force exhibited a progressive downward gradient from the root to the top of the peanut vine.

Table 3 Mean and standard deviation of maximum shear force at the cutting point of peanut vines

Sample	Root		Middle		Top	
Sample type	Mean/N	SD/N	Mean/N	SD/N	Mean/N	SD/N
1	47.3137	1.7268	37.0577	3.7706	25.2573	1.2046
2	46.5397	1.8913	33.3447	1.3885	26.1397	2.8291
3	48.1183	3.3142	35.5580	3.1186	24.7507	2.4616
4	43.7800	1.6970	35.2183	2.0505	25.1460	3.0748
5	46.4613	2.0369	36.4657	4.0193	25.1313	1.3462
Overall (n=25)	46.4426	1.7023	35.5289	1.4082	25.2850	0.5101

Based on the data visualization, Figure 7 presents a bar chart illustrating shear force errors at different shear locations on peanut vines. This chart clearly demonstrates the significant variations and patterns in shear mechanical properties across different plant sections. The error bars for each section are small and well-separated, indicating good consistency and reliability of the data. Among these, the peanut vine root section exhibited the smallest standard deviation, suggesting its structure was the most uniform and stable. In summary, the shear performance of peanut vines showed a gradual decline from root to top. Therefore, the specific section of the peanut vine significantly influenced the magnitude of the shear force applied.

3.3 Effect of moisture content in different parts of peanut vines on their shear force

The Q-Q plots of the normal distribution of moisture content in different parts of peanut vines are shown in Figure 8. In the plots (Figures 8a and 8c), the expected normal values for both the roots and tops fall within the upper and lower limits of the 95% confidence interval. Furthermore, these values are distributed on both sides of the line $y=x$, indicating that the measured moisture content values for the roots and tops of peanut vines conform to a normal distribution. In Figure 8b, one value lies outside the 95% confidence interval, while all other expected normal values stay within the interval and scatter on both sides of the line $y=x$. This indicates that the distribution characteristics of the measured values for the middle section of peanut vines differ slightly from a normal distribution.

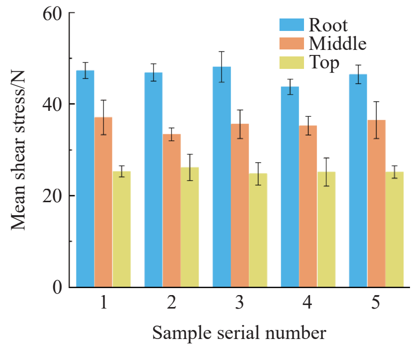

Figure 7 Peanut vine cutting position error bar chart

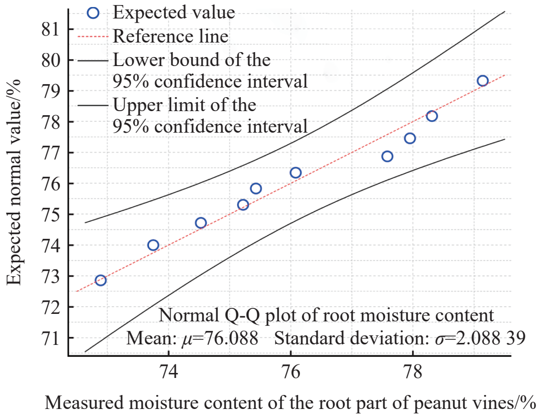

a. Q-Q plot of the root moisture content of peanut vines

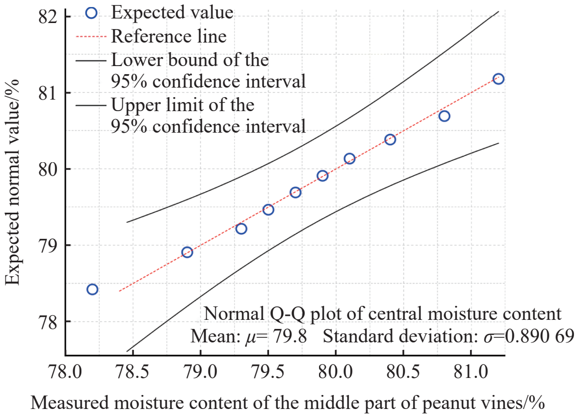

b. Q-Q plot of the middle moisture content of peanut vines

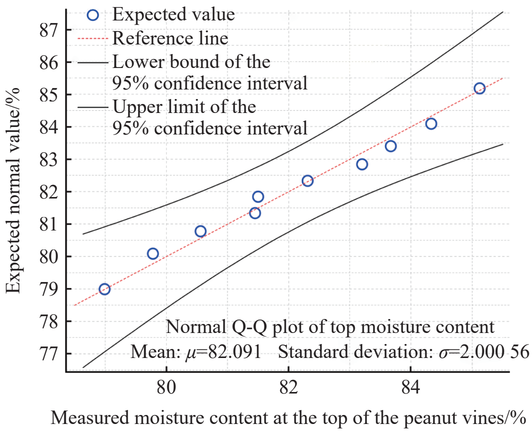

c. Q-Q plot of the top moisture content of peanut vines

Figure 8 Q-Q plot of normal distribution of moisture content in different parts of peanut vines

Measurements of moisture content in different parts of peanut vines indicate that the root section exhibits moisture levels ranging from 73.75% to 79.14%, with an average of 76.09%. The middle section showed moisture content between 78.2% and 81.2%, significantly higher than that of the roots. The maximum moisture content of the top section was 84.33%, with a minimum of 78.99% and an average of 82.09%. This section exhibited the highest moisture content among all parts.

After controlling peanut vine moisture content at 30%, 40%, and 50%, shear tests were conducted on the three moisture levels. The resulting shear curves, as shown in Figure 9, clearly revealed the significant impact of moisture content on their shear mechanical properties. From the curve profiles, all specimens exhibited typical elastic-plastic deformation characteristics: during the initial stage, shear stress increased approximately linearly with displacement, representing the elastic deformation phase. Subsequently, the specimens entered the plastic flow stage, where shear stress growth slowed until reaching a peak. Following the peak, shear failure occurred within the peanut vine structure, causing a rapid decline in load-bearing capacity.

Analysis of the test results showed that peanut vine exhibited the highest shear force at a moisture content of 30%, with a peak shear force of approximately 30.89 N. As moisture content increased to 40% and 50%, the material's peak shear force decreased to 25.71 N and 20.08 N respectively, demonstrating a clear, regular decreasing trend. This phenomenon clearly demonstrated that moisture had penetrated the cell walls of peanut vine fibers, weakening the inter-fiber bonding strength and consequently reducing the overall shear strength of the plant material. The curve profiles also revealed that specimens with higher moisture content exhibit flatter peak shapes, indicating increased toughness—particularly evident during the plastic deformation stage. This clearly confirms a negative correlation between moisture content and mechanical properties.

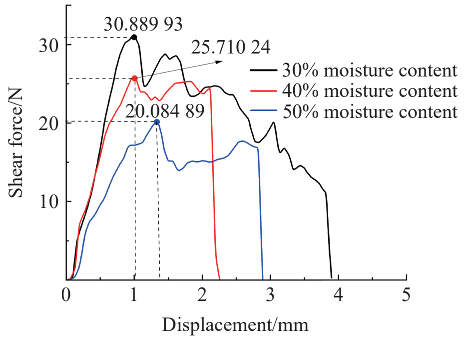

Figure 9 Shear force-displacement curve of peanut vines at different moisture contents

3.4 Ultimate load, fracture strength, and elastic modulus of peanut vines at different compression locations

Compression specimens measuring 15.00±0.05 mm in length were prepared from the root, middle, and top sections of peanut vines. Each specimen underwent 10 compression tests, yielding the compression curve shown in Figure 10. The obtained data were averaged, with results processed as listed in Table 4.

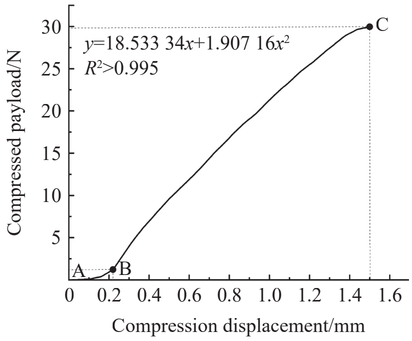

Figure 10 Peanut plant compression load-displacement curve

Table 4 Compressive mechanical properties parameters of different parts of peanut vines

Compression site	Ultimate load/N	Breaking strength/ MPa	Modulus of elasticity/MPa
Root	26.9012	0.391 85	3.5237
Middle	20.9443	0.281 88	2.6159
Top	15.6820	0.223 88	2.4490

Analysis of Figure 10 reveals that the compression load-displacement curve of peanut vines exhibits a two-stage deformation characteristic. During the elastic stage (segment AB), load and displacement showed an approximately linear relationship, indicating linear elastic deformation (R^2>0.995). In this stage, the stem structure of peanut vines primarily underwent recoverable elastic deformation, allowing it to largely return to its original state upon unloading.

When the compression displacement reaches point B, the curve enters the compression stage (segment BC). At this point, the slope of the curve increased significantly, and the load rose sharply with displacement, indicating that compression had begun within the pith cavity of the peanut vine. The onset of the point B compression stage marks a rapid compression deformation of peanut vines as displacement increases. During this phase, the hollow structure of the vines was compressed, causing their density to continuously increase and consequently boosting their compressive strength. Therefore, the compressive load corresponding to point C was the ultimate compressive load.

As shown in Table 4, among the ultimate load, breaking strength, and elastic modulus of different parts of peanut vines, the root section exhibited higher average values for all parameters compared to the middle and top sections. The ultimate load at the root section in the table was 26.90 N, with a fracture strength of 0.39 MPa and an elastic modulus of 3.52 MPa. This indicated that the root section exhibited greater structural toughness and could withstand higher compressive loads. In contrast, the mechanical properties of the peanut vine top were the weakest, with a maximum load of 15.68 N, a breaking strength of 0.22 MPa, and an elastic modulus of 2.45 MPa. This indicated that the top of the peanut vine was more prone to damage under compression. From this perspective, the compressive strength of peanut vines showed a gradual increase from the top to the roots.

3.5 Orthogonal experiment and response surface analysis

Shear tests were conducted on peanut vine specimens at different sampling locations, loading rates, and moisture contents[33,34]. Based on this, orthogonal experiments and analysis of variance were conducted to establish a second-order response model for the shear force F_N of peanut vine, considering different sampling positions A, loading rates B, and moisture contents C. The experimental factors and their level codes are listed in Table 5, and the influence of interaction terms on the mechanical properties of peanut vine was analyzed.

Table 5 Trial factors and level coding table

Factor level	Sampling locations (A)	Loading rates (B)/ mm·min^{-1}	Moisture contents (C)/%
1	Bottom	50	50
0	Middle	40	40
–1	Top	30	30

Using Design Expert 13 software, a Box-Behnken design was employed to create 17 experimental combinations, as shown in Table 6. A multiple regression model was established to relate each factor to the shear force Y.

Table 6 Shear force orthogonal test plan and results

Test number	Experimental factors			Test indicators
	A	B	C	Shear force/N
1	1	–1	0	29.8
2	–1	–1	0	12.5
3	1	1	0	26.4
4	–1	1	0	14.2
5	1	0	–1	32.1
6	–1	0	–1	16.3
7	1	0	1	24.6
8	–1	0	1	11.7
9	0	–1	–1	27.9
10	0	1	–1	28.5
11	0	–1	1	20.3
12	0	1	1	18.2
13	0	0	0	21.5
14	0	0	0	19.8
15	0	0	0	22.1
16	0	0	0	20.9
17	0	0	0	21.2

Table 7 presents the results of the analysis of variance (ANOVA) for the orthogonal design of the shear force Y on peanut vines. Analysis of the data in Table 7 indicates that the main effects of A ($p<1\times10^{-4}$), C ($p<1\times10^{-4}$) are highly significant factors influencing the shear force F_N of peanut vines. The interaction terms AB ($0.01<p=0.0400<0.05$), interaction term A^2 ($0.01<p=0.0211<0.05$), and interaction term C^2 ($0.01<p=0.0170<0.05$) were significant factors affecting the shear force F_N of peanut vines. The p-values for the remaining factors were all greater than 0.05, therefore they were determined to be non-significant factors. The most significant factors affecting the shear force F_N of peanut vines and their order of significance are as follows: $A>C>C^2>A^2>AB$.

Table 7 Box-Behnken design ANOVA table for peanut vine shear force

Source	Sum of squares	*df*	Mean square	*F*-value	*p*-value
Model	570.67	9	63.41	61.73	<0.0001**
A	423.41	1	423.41	412.22	<0.0001**
B	1.28	1	1.28	1.25	0.3011
C	112.50	1	112.50	109.53	<0.0001**
AB	6.50	1	6.50	6.33	0.0400*
AC	2.10	1	2.10	2.05	0.1956
BC	1.82	1	1.82	1.77	0.2246
A^2	9.01	1	9.01	8.77	0.0211*
B^2	4.98	1	4.98	4.85	0.0636
C^2	9.95	1	9.95	9.69	0.0170*
Residual	7.19	7	1.03	-	-
Lack of fit	4.29	3	1.43	1.97	0.2603
Pure error	2.90	4	0.7250	-	-
Cor total	577.86	16	-	-	-

Note：** indicates a highly significant factor, $p\leq0.01$; * indicates significant factors, $0.01<p\leq0.05$; $p>0.05$ is non-significant factors.

Based on the results of the regression analysis of variance and the coding factors, a quadratic response model was established to describe the relationship between the shear force of peanut vines and the sampling locations, loading rates, and moisture contents, as shown in Equation (7):

$$Y = 21.10 + 7.28A - 0.4B - 3.75C - 1.28AB - 0.725AC - 0.675BC - 1.46A^2 + 1.09B^2 + 1.54C^2 \quad (7)$$

Considering only the effects of highly significant factors and significant factors on the second-order response model, Equation (7) can be further simplified to Equation (8):

$$Y = 21.10 + 7.28A - 3.75C - 1.28AB - 1.46A^2 + 1.54C^2 \quad (8)$$

Response surfaces and contour plots provide a visual representation of the extent to which interactions affect the response values. The steeper the surface and the denser the contour lines, the more significant the effect; the closer the contour lines are to an ellipse, the stronger the interaction between the two factors[35].

Figure 11 illustrates the influence of the interaction term AB on the shear force Y of the peanut vine when the moisture contents C is at the central level of 0. The response surface in the figure illustrates the influence of the interaction between sampling locations A and loading rates B on the shear force Y of peanut vines, with other factors held at the central level. When the loading rates B is fixed, the shear force Y shows a significant upward trend as the level of sampling locations A changes from –1 to 1; this promoting effect of A on shear force is more pronounced at higher loading rates. When the sampling locations A is fixed, the shear force Y also increases as the level of loading rates B changes from –1 to 1, with a greater increase in shear force when A is at a high level. The slope of the response surface is steeper along the A direction than along the B direction, indicating that sampling locations A has a stronger effect on shear force than loading rates B. In addition, the contour lines at the bottom show a distinct non-parallel pattern, further demonstrating a significant interaction between A and B, which is consistent with the significant result for the AB term in the analysis of variance.

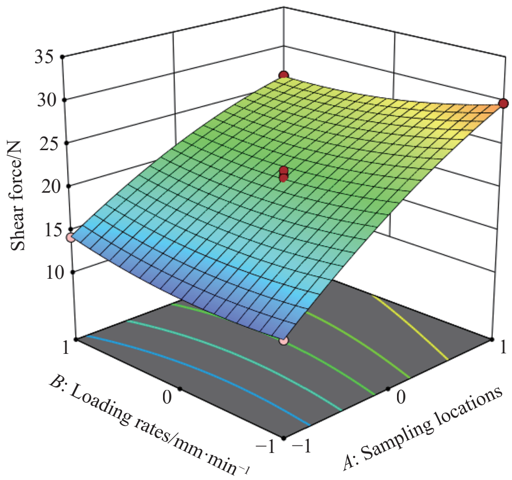

Figure 11 Relation of interaction term AB vs. shear force F_N

Figure 12 shows the response surfaces of the AC interaction term and the BC interaction term on the shear force of peanut vines. Although the figure reveals certain trends in the response surfaces, the results of the analysis of variance indicate that neither the AC interaction term nor the BC interaction term had a significant effect on the shear force. This indicates that, under the experimental conditions of this study, the interactions between sampling locations and loading rates, and between shear position and moisture contents, do not significantly affect the shear force; the effects of each factor on the shear force are primarily manifested as independent main effects.

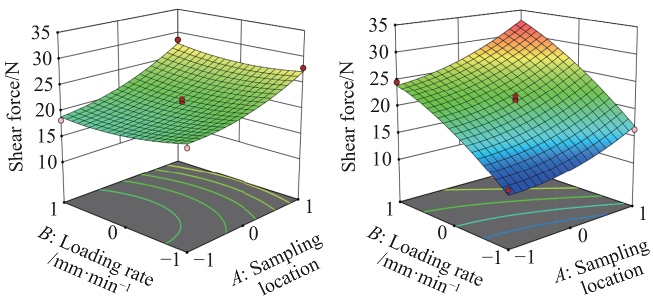

a. Interaction term BC b. Interaction term AC

Figure 12 Response surface plots for the non-significant interaction terms

Although the response surface analysis identified sampling location and moisture content as the dominant factors affecting shear force, the loading rate still exhibited a positive effect within the quasi-static range. Increasing the loading rate from 30 to 50 mm/min resulted in an approximately 65% increase in the average maximum shear force.

4 Conclusions

This study employed peanut vines collected in Henan Province as test specimens. Shear and compression tests were conducted using a universal testing machine. Response surface methodology was applied, with sampling location, loading rate, and moisture content serving as factors, and shear force as the response indicator. The analysis examined the influence patterns of these factors on the mechanical properties of peanut vines. The research findings were as follows:

1) Shear tests were conducted to characterize the mechanical properties of peanut vines. Increasing the loading rate from 30 to 50 mm/min resulted in a higher maximum shear force. Among different sampling locations, the mean maximum shear forces at the root, middle, and top sections were 46.44±1.70 N, 35.53±1.41 N, and 25.29±0.51 N, respectively, showing a decreasing trend from the root to the top. Shear force-displacement curves exhibited a bimodal characteristic, indicating that peanut vines undergo two distinct mechanical response stages during shearing: the outer skin and the pith cavity. At different moisture contents, higher moisture content resulted in lower shear force in peanut vines.

2) Through compression testing of peanut vines, it was found that the root section exhibits the most outstanding mechanical properties, with significantly higher average ultimate load, fracture strength, and elastic modulus compared to the middle and top sections. This indicated that from the top to the root of the vine, the vine's resistance to compressive deformation and load-bearing capacity progressively increases as its structure becomes denser and the proportion of pith cavities relatively decreases. This pattern corroborated the findings from shear tests, where the root section exhibited the strongest shear resistance. Together, these results demonstrated that the root section of peanut vines possesses the most resilient mechanical structure.

3) Using response surface methodology to perform variance analysis on peanut vine cutting test results revealed that sampling location and moisture content were highly significant factors affecting peanut vine cutting. Under the conditions of the shear location at the root, a loading rate of 40 mm/min, and a moisture content of 30%, the combination yielding the maximum shear force under quasi-static conditions was identified. These results provide baseline quasi-static mechanical properties, while the mechanical response under high-speed dynamic impact remains to be investigated in future work.

Acknowledgements

This study was supported by the Natural Science Foundation of Henan Province (Grant No. 252300421922), the Henan Provincial Key Research and Development Program (Grant No. 261111111200 and No. 241111111300), and the National Natural Science Foundation of China (Grant No. 52265037).

[References]

[1] Yuan Y L, Zhen Z G, Zhang J P, Zhu Y J, Wang X L, Cui J M, et al. Innovations and prospects of summer peanut cultivation technology in Henan Province. China Seed Industry, 2025(12): 33–37. (in Chinese)

[2] Yang M, Zhang Y H, Zhang C, Gu F W, Yu Z Y, Hu Z C. Design and experiment of fan-sieve combined peanut film seedling separating device based on shredding and separating. Transactions of the CSAM, 2020; 51(12): 112–121. (in Chinese)

[3] He X N, Li M Z, Chang X L, Shang S Q, Wang D W, Wang J S, et al. Design and experiment of LS-DYNA-based disk-type peanut root-cutting device. Transactions of the CSAE, 2025; 41(21): 32–42. (in Chinese)

[4] Zhao X Y, Chen J, Du F L. Potential use of peanut by-products in food processing: A review. Journal of Food Science and Technology, 2012; 49: 521–529.

[5] Zeng B, Tang M, Tang W, Yu G Y, Zeng J Q. Research progress of peanut meal and peanut straw in animal feeding. China Feed, 2023(5): 152–162. (in Chinese)

[6] Yan L M, Wu T, Jiang D L, Gou H X, Fu X H, Zhang J H. Design and experiment of side-throwing cotton stalk crushing and returning device. Transactions of the CSAM, 2025; 56(3): 216–226. (in Chinese)

[7] Başlar M, Kalkan F, Kara M, Ertugay M F. Correlation between the protein content and mechanical properties of wheat. Turkish Journal of Agriculture and Forestry, 2012; 36(5): 601–607.

[8] Li W X, Zhang F B, Luo Z T, Zheng E L, Pan D C, Qian J, et al. Straw movement and flow field in a crushing device based on CFD-DEM coupling with flexible hollow straw model. Biosystems Engineering, 2024; 242: 140–153.

[9] Shen H Y, Luo W W, Wu F, Gu F W, Yang H G, Hu Z C. Research progress on mechanized harvesting equipment and technology for peanuts. Transactions of the CSAM, 2024; 55(8): 21–38. (in Chinese)

[10] Gu F W, Zhao Y Q, Hu Z C, Shi L L, Wu F, Xu H B, et al. Operation analysis and parameter optimization of the conveying device for uniform crushed straw throwing and seed-sowing machines. Int J Agric & Biol Eng, 2023; 16(6): 28–36.

[11] Wu K, Song Y P. Research progress analysis of crop stalk cutting theory and method. Transactions of the CSAM, 2022; 53(6): 1–20. (in Chinese)

[12] Chahal A, Ciolkosz D, Puri V, Jacobson M, Liu J. Mechanical characteristics of wood-bark interface of shrub willow. Industrial Crops and Products, 2021; 162: 113236.

[13] Shi Y Y, Chen M, Wang X C, Zhang Y N, Odhiambo M O. Experiment and analysis on mechanical properties of Artemisia selengensis stalk. Int J Agric & Biol Eng, 2017; 10(2): 16–25.

[14] Ye D P, Qing J X, Lin Z Q, Wu Y T, Lai H K, Weng H Y. Establishment and parameter calibration of discrete element model for neyraudia reynaudiana stalk. Transactions of the CSAM, 2025; 56(7): 139–149. (in Chinese)

[15] He X, Peng Q G, Li G M, Wang X Y, Zhang C Y, Kang J M. Experiment on determination of recovery coefficient of peanut seedling. Transactions of the CSAM, 2024; 55(S1): 156–164. (in Chinese)

[16] Liu Y G, Zhao J G, Yin B Z, Ma Z K, Hao J J, Yang X, et al. Discrete element modelling of the yam root–soil complex and its verification. Biosystems Engineering, 2022; 220: 55–72.

[17] Coetzee C J, Els D N J. Calibration of discrete element parameters and the modelling of silo discharge and bucket filling. Computers and Electronics in Agriculture, 2009; 65: 198–212.

[18] Ma X J, Yu Z H, Liu M, Wang J L, Su Q, Zhang Z C, et al. Mechanical properties and critical state characteristics of maize root-soil composites at different soil depths. Biosystems Engineering, 2025; 250: 163–173.

[19] Schramm M, Tekeste M Z. Wheat straw direct shear simulation using discrete element method of fibrous bonded model. Biosystems Engineering, 2022; 213: 1–12.

[20] Chen P Y, Jia F G, Zhang Z C, Han Y L, Li A Q, Wang Y L, et al. Breakage mechanism of brown rice grain during rubber roll hulling. Biosystems Engineering, 2023; 225: 41–53.

[21] Liang R Q, Chen X G, Zhang B C, Wang X Z, Kan Z, Meng H W. Calibration and test of the contact parameters for chopped cotton stems based on discrete element method. Int J Agric & Biol Eng, 2022; 15(5): 1–8.

[22] Zhang Y Z, Zhou L, Zhao H B, Liu J J, Qin W H, Zhao H C, et al. Analysis of shear mechanical properties of tobacco apical bud stalks. Tobacco Science and Technology, 2025; 58(3): 32–40. (in Chinese)

[23] Li Y D, Du X J, Song Z H, Li F D. Test of shear mechanical properties of cotton stalks. Transactions of the CSAE, 2011; 27(2): 124–128. (in Chinese)

[24] Hirai Y, Inoue E, Mori K, Hashiguchi K. PM—Power and machinery: Investigation of mechanical interaction between a combine harvester reel and crop stalks. Biosystems Engineering, 2022; 83(3): 307–317.

[25] Shen Z H, Dong Z K, Chen W W, Xia A Q, Cao W H. Study of shearing properties of sugarcane buds. Journal of Agricultural Mechanization Research, 2024; 46(4): 145–152. (in Chinese)

[26] Liang R Q, Zhang L P, Jia R, Meng H W, Kan Z, Zhang B C, et al. Study on friction characteristics between cotton stalk-residual film-external contact materials. Industrial Crops and Products, 2024; 209: 118022.

[27] Zhang S W, Sun Y Y, Zhang Y J, Dai M, Miao H, Zhang Y J, et al. Experimental study on the biomechanical characteristics of millet pepper. Journal of Agricultural Mechanization Research, 2025; 47(4): 151–159. (in

Chinese)

[28] Wang Y F, Yasir M, Walayat N, Ahmed I A M, Zhang W, Zheng J, et al. Exploring the impact of diverse combinations of withering methods and drying temperatures on the quality characteristics of white tea. Industrial Crops and Products, 2025; 237: 122196.

[29] Wang H C, Xia J J, Dong Z, Liu L L, Wang T, Zhang G Z. Mechanical properties of compression in Zizania latifolia. Journal of Huazhong Agricultural University, 2025; 44(4): 280–287. (in Chinese)

[30] Li T Y, Guan X D, Zhou F J. Mechanistic analysis and experimental study of a shear-type low-loss fresh corn ear-picking mechanism. Computers and Electronics in Agriculture, 2023; 213: 108191.

[31] Shen Y Y, Fang B, Huang J W, Liu Y Q, Ye D P, Xie L M. Experimental study on morphology and mechanical properties of Pleurotus eryngii. Journal of Chinese Agricultural Mechanization, 2025; 46(2): 147–152. (in Chinese)

[32] Ma X L, Xu F Y, Liu Z. A method for evaluation of the probability density function of white noise filtered non-Gaussian stochastic process. Mechanical Systems and Signal Processing, 2024; 211: 111242.

[33] Liang R Q, Chen X G, Zhang B C, Peng X B, Meng H W, Jiang P, et al. Tests and analyses on mechanical characteristics of dwarf-dense-early major cotton variety stalks. International Agrophysics, 2020; 34: 333–342.

[34] Liang R Q, Zhang B C, Zhou P F, Li Y P, Meng H W, Kan Z. Power consumption analysis of the multi-edge toothed device for shredding the residual film and impurity mixture. Computers and Electronics in Agriculture, 2022; 196: 106898.

[35] Li J P, Ren J Z, Chen Y H, Feng Q G. Optimization of top comb process parameters in cotton combing based on response surface methodology. Cotton Textile Technology, 2026. (in Chinese) doi: 10.26967/j.issn1000-7415.202602010.